



HAL
open science

Self-Cleaning Interfaces of Polydimethylsiloxane Grafted with pH-Responsive Zwitterionic Copolymers

Jacqueline S. de Vera, Antoine Venault, Ying-Nien Chou, Lemmuel Tayo, Heng-Chieh Chiang, Pierre Aimar, Yung Chang

► **To cite this version:**

Jacqueline S. de Vera, Antoine Venault, Ying-Nien Chou, Lemmuel Tayo, Heng-Chieh Chiang, et al.. Self-Cleaning Interfaces of Polydimethylsiloxane Grafted with pH-Responsive Zwitterionic Copolymers. *Langmuir*, 2019, 35 (5), pp.1357-1368. 10.1021/acs.langmuir.8b01569 . hal-02305398

HAL Id: hal-02305398

<https://hal.science/hal-02305398v1>

Submitted on 4 Oct 2019

HAL is a multi-disciplinary open access archive for the deposit and dissemination of scientific research documents, whether they are published or not. The documents may come from teaching and research institutions in France or abroad, or from public or private research centers.

L'archive ouverte pluridisciplinaire **HAL**, est destinée au dépôt et à la diffusion de documents scientifiques de niveau recherche, publiés ou non, émanant des établissements d'enseignement et de recherche français ou étrangers, des laboratoires publics ou privés.



Open Archive Toulouse Archive Ouverte

OATAO is an open access repository that collects the work of Toulouse researchers and makes it freely available over the web where possible

This is an author's version published in: <http://oatao.univ-toulouse.fr/24262>

Official URL:

<https://doi.org/10.1021/acs.langmuir.8b01569>

To cite this version:

De Vera, Jacqueline S. and Venault, Antoine and Chou, Ying-Nien and Tayo, Lemmuell and Chiang, Heng-Chieh and Aimar, Pierre and Chang, Yung *Self-Cleaning Interfaces of Polydimethylsiloxane Grafted with pH-Responsive Zwitterionic Copolymers*. (2019) *Langmuir*, 35 (5). 1357-1368. ISSN 0743-7463

Any correspondence concerning this service should be sent to the repository administrator: tech-oatao@listes-diff.inp-toulouse.fr

Self-Cleaning Interfaces of Polydimethylsiloxane Grafted with pH-Responsive Zwitterionic Copolymers

Jacqueline S. De Vera,^{†,‡} Antoine Venault,[†] Ying-Nien Chou,[†] Lemmuel Tayo,[‡] Heng-Chieh Chiang,[§] Pierre Aimar,^{||} and Yung Chang^{*,†}

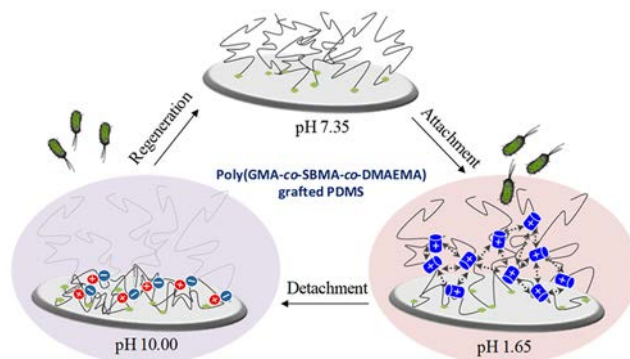
[†]R&D Center for Membrane Technology and Department of Chemical Engineering, Chung Yuan Christian University, Chung-Li, Taoyuan 320, Taiwan

[‡]School of Chemical, Biological and Materials Engineering and Sciences, Mapua University, Intramuros, Muralla St., Manila 1002, Philippines

[§]Division of Urology, Department of Surgery, Changhua Christian Hospital, 135 Nanxian St., Changhua 500, Taiwan

^{||}Laboratoire de Génie Chimique, Université Paul Sabatier, 118 route de Narbonne, 31062 Toulouse Cedex 9, France

ABSTRACT: Self-cleaning surfaces allow the reversible attachment and detachment of microorganisms which show great promise in regards to their reusability as smart biomaterials. However, a widely used biomaterial such as polydimethylsiloxane (PDMS) suffers from high biofouling activity and hydrophobic recovery that results in decreased efficiency and stability. A current challenge is to modify and fabricate self-cleaning PDMS surfaces by incorporating antifouling and pH-sensitive properties. To address this, we synthesized a zwitterionic and pH-sensitive random poly-(glycidyl methacrylate-*co*-sulfobetaine methacrylate-*co*-2-(dimethylamino)ethyl methacrylate) polymer, poly(GMA-*co*-SBMA-*co*-DMAEMA). In this work, chemical modification of PDMS was done by grafting *onto* poly(GMA-*co*-SBMA-*co*-DMAEMA) after surface activation via UV and ozone for 90 min to ensure the formation of covalent bonds necessary for stable grafting. The PDMS grafted with G20-S40-D40 exhibit antifouling and pH-sensitive properties by mitigating fibrinogen adsorption, blood cell adhesion, and releasing 98% adhered *E. coli* bacteria after immersion at basic pH. The grafting of poly(GMA-*co*-SBMA-*co*-DMAEMA) presented in this work shows attractive potential for biomedical and industrial applications as a simple, smart, and effective method for the modification of PDMS interfaces.



■ INTRODUCTION

Polydimethylsiloxane (PDMS) is a desirable biomaterial for its biocompatibility, optical transparency, ease of fabrication and low cost.¹ However, PDMS suffers from high biofouling of nonspecific adsorption of cells, proteins, and microorganisms which is attributed to its low wettability and hydrophobicity, thus posing a problem in terms of device efficacy and safety.^{2,3} Biofouling or fouling is the nonspecific adsorption of proteins, cells, and microorganism onto the material surface.⁴⁻⁶ The uncontrolled adhesion of biological compounds on the surface of implant materials is a harmful phenomenon that causes the function of biomedical devices to deteriorate. For example, fouling can block the material surface of contact lenses,⁷⁻⁹ surface plasmon resonance (SPR) sensors,^{10,11} or prevent the release of drugs from MEMS-based devices.¹²⁻¹⁴

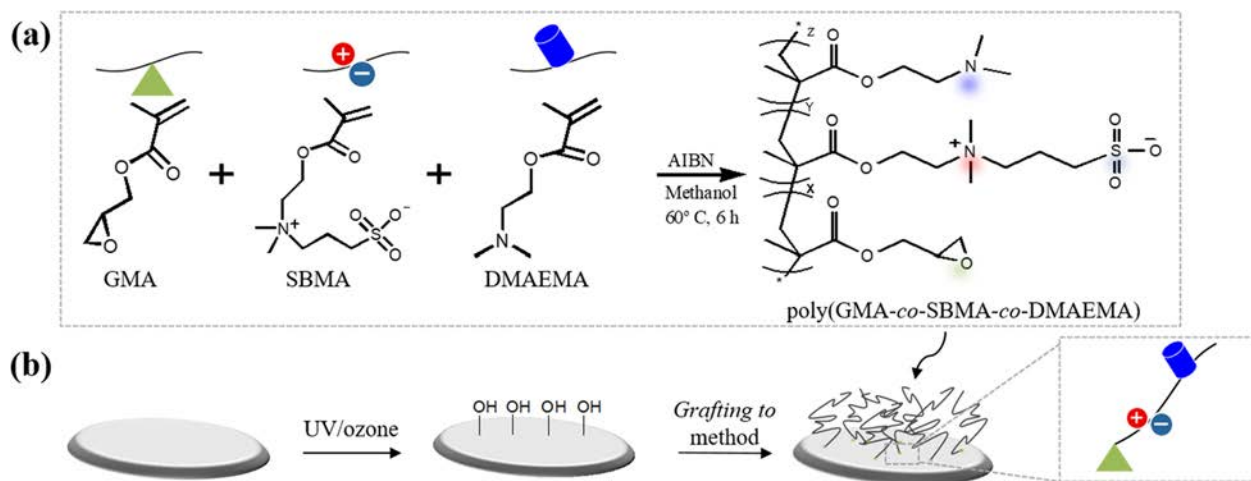
Low fouling can be achieved by chemically modifying the surface via coating of hydrophilic materials like poly(ethylene glycol) (PEG) systems or zwitterionic polymers. However, PEGylated systems suffer from chemical instability in complex media,¹⁵ unlike zwitterionic polymers. By definition, zwitter-

ionic polymers have a net charge of zero with equimolar amounts of cationic and anionic groups in their polymer chain.¹⁶ A famous zwitterionic polymer is phosphorylcholine (PC) in which the zwitterion is formed by the association of a phosphate anion and a quaternary ammonium cation. In particular, the methacrylate phosphorylcholine (MPC) is among the most popular PC derivatives, and its synthesis in 1990 opened the door to countless antifouling, hemocompatible and biocompatible surface designs.¹⁷ The main disadvantage of methacrylate phosphorylcholine (MPC) polymers is their complex synthetic route and low yield. Another zwitterionic polymer, poly(sulfobetaine methacrylate) (PSBMA) has become popular when grafted to surfaces because it reduces fouling of plasma proteins and blood

Table 1. Theoretical and Actual Compositions of the Copolymers and Their Particle Size

sample ID	composition in feed (mol %) ^a			composition in polymer (mol %) ^b			yield (%)	particle size (nm)
	GMA	SBMA	DMAEMA	GMA	SBMA	DMAEMA		
G20-D80	20		80	21		79	69.4	193.7
G20-S25-D55	20	25	55	17	25	58	58.2	192.4
G20-S40-D40	20	40	40	17	41	42	61.9	409.6
G20-S55-D25	20	55	25	17	58	25	62.8	134.2
G20-S80	20	80		23	77		75.6	<10

^aTheoretical mole fraction of reacted monomers for copolymer synthesis. ^bMole fraction of copolymers were determined by ¹H NMR.

Scheme 1^a

^a(a) Reaction scheme for the random copolymerization of copolymer poly(GMA-co-SBMA-co-DMAEMA) and (b) grafting of poly(GMA-co-SBMA-co-DMAEMA) on PDMS.

cells.^{18,19} In addition, SBMA has been shown to be easily synthesized with a controlled chain length, and its synthesis led to higher yields, compared to zwitterionic MPCs. Also, thanks to its ease of production, applicability and bioinert nature attributed to the formation of a strong hydration layer, PSBMA and its derivatives have become first choice materials in the design of antifouling surfaces.^{20,21} Generally, low fouling can be achieved by using grafting *to* approach to chemically modify the surface via coating of hydrophilic materials. The grafting consists of a reactive chain end on the substrate followed by chemisorption of the copolymer to produce a stable zwitterionic surface.²²

Despite the beneficial use of zwitterionic polymers in preventing fouling, incorporating these polymers for biosensors with bacterial detection and monitoring functions such as in microfluidic single-cell analysis is not applicable because contact with the surface material is necessary for analysis of bacteria culture.^{23–25} Single-cell analysis is an interesting field as it holds potential in studying the intrinsic behavior of microorganisms like *Escherichia coli*.²⁶ Therefore, the concentration of microorganisms such as bacteria on the sensor surface should be regulated to prevent fouling and to maximize the reusability of the sensor. A promising approach for this is to use self-cleaning property by switching from bacteria-adhering to bacteria-releasing surface by taking advantage of the change in surface morphology and hydrophilicity.^{27–29} Self-cleaning surfaces exploit the dynamics of drop formation and wetting to maximize the removal of foulants when doused with an aqueous solvent.^{30,31}

This study aims to design a self-cleaning PDMS surface. It involves the introduction of a copolymer made of anchoring glycidyl methacrylate (GMA) segments, antifouling sulfobetaine methacrylate (SBMA) segments, and pH-responsive 2-(dimethylamino)ethyl methacrylate (DMAEMA) segments, poly(GMA-co-SBMA-co-DMAEMA). Functionalization with DMAEMA moieties can permit one to obtain a self-cleaning surface exhibiting reversible attachment and release of bacteria from the material surface after changes in pH.^{32,33} In addition, to ensure successful cross-linking of the design polymer onto the PDMS surface, the use of epoxide functional groups (GMA) which opening is catalyzed by a basic agent (ring-opening reaction), leads to the formation of covalent bonds with the material surface.³⁴ Our polymer, containing cross-linking units, antifouling units, and stimuli-responsive units, grafted onto a PDMS surface leads to the formation of a self-cleaning interface that could be applied in biosensors for bacterial monitoring and detection.

■ EXPERIMENTAL SECTION

Materials. Sulfobetaine methacrylate (SBMA) was purchased from HOPAX. Glycidyl methacrylate (GMA), 2-(dimethylamino)ethyl methacrylate (DMAEMA), azobis(isobutyronitrile) (AIBN), and triethylamine (TEA) were purchased from Sigma-Aldrich. Human plasma fibrinogen (fraction I), primary monoclonal antibody, and secondary monoclonal antibody were purchased from Sigma Chemical Co. US. Deionized water (DI water) was purified using the Millipore water purification system with a minimum resistivity of 18.0 MΩ·cm. Lastly, the substrate used was Sylgard 184 PDMS which was purchased from Dow Corning with components supplied in two parts, the Sylgard 184A prepolymer and Sylgard 184B curing agent.

Synthesis and Chemical Characterization of Poly(GMA-co-SBMA-co-DMAEMA) Copolymers. Different polymer solutions of poly(GMA-co-SBMA-co-DMAEMA) with a solid content of 20% (w/w) were prepared with methanol and water with a volume ratio of 3:1. The solutions were purged with N₂ gas and stirred for the next 10 min. To start the free radical polymerization process, the initiator AIBN was added and dissolved for another 10 min, then heated for 6 h at 60 °C with constant stirring. The purification of the polymer was carried out by addition of IPA and the precipitate obtained was freeze-dried for 48 h. For the controls, antifouling zwitterionic poly(GMA-co-SBMA) and pH-responsive poly(GMA-co-DMAEMA) were also synthesized using the same methods stated above. The chemical structure and composition of the copolymers and controls are presented in Table 1 and Scheme 1, respectively. Furthermore, the chemical structure of the poly(GMA-co-SBMA-co-DMAEMA) copolymer was characterized by ¹H NMR spectra with a 500 MHz Bruker spectrometer using D-methanol as the solvent. Finally, although visually transparent solutions were obtained, indicating apparent solubility of the poly(GMA-co-SBMA-co-DMAEMA) copolymers in aqueous solvents, characteristic particle sizes remained too large to assess molecular weights. Thus, we only report in Table 1 particle sizes of the different copolymers assessed with a dynamic light scattering instrument (DelsaTM Nano S, Beckman Coulter).

Preparation and Surface Characterization of Self-Assembled Poly(GMA-co-SBMA-co-DMAEMA) Interfaces via Grafting to Method. A 10:1 ratio of Sylgard 184A/Sylgard 184B mixture was prepared and stirred in a small beaker using a glass rod. The trapped bubbles were removed by ultrasonication for 30 min. Then, the mixture was cast into a clean flat glass Petri dish and cured for 24 h at room temperature. The cured substrates (≈3 mm thick) were cut into circles with a diameter of 10 mm. Finally, the substrates were dried with N₂ gas and stored in vacuum containers to avoid possible contamination.

The optimized pretreatment time and coating concentration for the surface activation of PDMS substrates using ultraviolet (UV) light ozone cleaner was determined by verifying the change in the hydrophilicity of the virgin PDMS surface when at a source power of 110 W with the help of a contact angle goniometer (Automatic Contact Angle Meter, model CA-VP, Kyowa Interface Science Co., Ltd., Japan). Enzyme-linked immunosorbent assay (ELISA) was also used to evaluate the surface fouling of the modified PDMS samples. The step-by-step procedure for ELISA is defined on the next section. Next, the treated substrates were immersed into different concentrations of aqueous poly(GMA-co-SBMA-co-DMAEMA) copolymer solution for 1 h by ultrasonication. In addition, 50 μL of triethylamine (TEA) was mixed into the coating solution and placed in an oven at 60 °C for 15 h. Finally, the grafted substrates were washed three times in DI water and immersed in phosphate buffered solution (PBS) and stored in an oven at 37 °C.

In addition, the chemical composition of surface modified PDMS membranes was determined with ATR-FTIR spectrophotometry (Bruker Tensor 27 FTIR) with ZnSe as reflection element. Each spectrum was captured by averaging 30 scans at a resolution of 4 cm⁻¹. Also, X-ray photoelectron spectroscopy measurements were conducted using a Thermo K-Alpha XPS System equipped with a monochromated Al K_α X-ray source (1,486.6 eV photons) to determine the elemental analysis of the grafted substrate in which the energy of the emitted electrons was measured at a range of 50–150 eV. Finally, zeta potential of the modified PDMS was measured by SurPASSTM electrokinetic analyzer. The PDMS samples having an area of 10 × 20 mm² were adjusted to the measuring cell wherein electrolytes with 0.1 M concentration each of KCl, KH₂PO₄, and NaHCO₃ were added. The pH was adjusted using 0.1 M of HCl and 0.1 M NaOH to measure streaming potential in different pH.

Fibrinogen Adsorption and Surface Wettability. ELISA was used to evaluate the adsorption of human fibrinogen onto the grafted substrates according to the protocol earlier reported and reminded here.³⁵ The grafted substrates were prepared in triplicates and immersed in individual wells with 1000 μL of PBS at 37 °C overnight to guarantee their stabilization. Next, the substrates were immersed in

1000 μL of fibrinogen solution at 37 °C for another hour and were rinsed in PBS solution thrice. Using the same parameters, bovine serum albumin (BSA), followed by primary monoclonal antibody, and again by addition of BSA, and finally horseradish peroxidase-conjugated secondary monoclonal antibody were added separately in series and allowed to react with the grafted substrates for 1 h and washed with PBS thrice. To ensure that the substrates were clean, the membranes were washed five times with PBS and transferred into clean wells before incubating with 500 μL of 3,3',5,5'-tetramethylbenzidine chromogen 0.05 wt % Tween 20, and 0.05 wt % hydrogen peroxide (TMB), for 8 min at 37 °C. To stop the enzymatic color reaction, 500 μL of 0.1 M sulfuric acid were added and the absorbance recorded at 450 nm using a UV-vis spectrophotometer (Power-Wave XS, BioteK). The positive and negative controls used were the SBMA hydrogel and tissue culture polystyrene (TCPS) well plate.

In addition, the surface wettability was assessed by measuring the average water contact angle in air of the samples at three different sites on the sample surface using an angle-meter (Automatic Contact Angle Meter, model CA-VP, Kyowa Interface Science Co., Ltd., Japan).

Blood Cells Adhesion. The hemocompatibility of the polymer grafted onto PDMS surface was determined using blood cell adhesion experiment wherein fresh blood samples were obtained from a pool of healthy volunteers. Blood coagulation was prevented by addition of ethylenediaminetetraacetic acid (EDTA). First, 1 mL of PBS was added to the grafted substrates overnight at 37 °C to promote stabilization. Next, the platelet-rich plasma (PRP) was obtained using a centrifuge set at 1200 rpm for 10 min. PRP was recalcified by addition of 5 μL of 1 M CaCl₂ followed by washing with PBS. Finally, immersion of substrates into 2.5% glutaraldehyde in PBS solution enabled the immobilization of the activated PRP onto the substrate.

The red blood cells concentrate (RBC) was obtained by the centrifugation of 250 mL fresh whole blood at 1200 rpm for 10 min. Stabilization of the wells were achieved by the addition of 1 mL of PBS for 24 h at 37 °C. Afterward, the substrates together with the RBC concentrates were placed in the wells and incubated for 120 min at 37 °C. In order to immobilize the cells onto the substrates, the substrates were washed with PBS twice and immersed in 300 μL of 2.5% glutaraldehyde in PBS solution for 10 h at 4 °C.

The adhesion of whole blood was studied similarly, by incubating the substrate in whole blood for 2 h at 37 °C. 2.5% glutaraldehyde in PBS solution was added for immobilization of cells on the surface.

For the analysis of blood cell adhesion, the substrates were observed at three various sites using a confocal laser scanning microscope (CLSM) (NIKON CLSM A1R) operated at a 200× magnification. The quantitative results were assessed using ImageJ cell counting software by taking the average results from three different areas for each condition.

Bacterial Attachment and Detachment at Different pH. To verify the self-cleaning property of poly(GMA-co-SBMA-co-DMAEMA) brushes upon pH changes, bacterial attachment and detachment of bacteria were investigated using the optimum ratio of the polymer that exhibits excellent antifouling property in terms of low relative fibrinogen adsorption, hydrophilic property as shown by its low water contact, and low blood cell component adhesion. It should also exhibit pH-responsive properties owing to changes in swelling ratio and varying bacterial cell density in acidic or basic conditions. A medium containing 3.0 mg/mL beef extract and 5.0 mg/mL peptone was used to culture the bacteria. The culture medium was then incubated at 37 °C and was shaken at 100 rpm for 12 h. The grafted substrates were immersed in pH 1.65 for 2 h at 37 °C. Then, 1 mL of bacterial solution was added to each well. The solution was removed after 1 h, and each sample was washed with their respective pH buffers for 3 times to remove any unattached bacteria. The substrates were observed using confocal laser scanning microscopy (CLSM) (NIKON CLSM A1R) with images taken at three different sites. After that, the grafted substrates were immersed in pH 7.35 for 30 min at 37 °C to observe any detached bacteria from the surface using CLSM. Lastly, the same substrates were washed with pH 10 buffer for three times and observed under the microscope. Because the charge-reversal

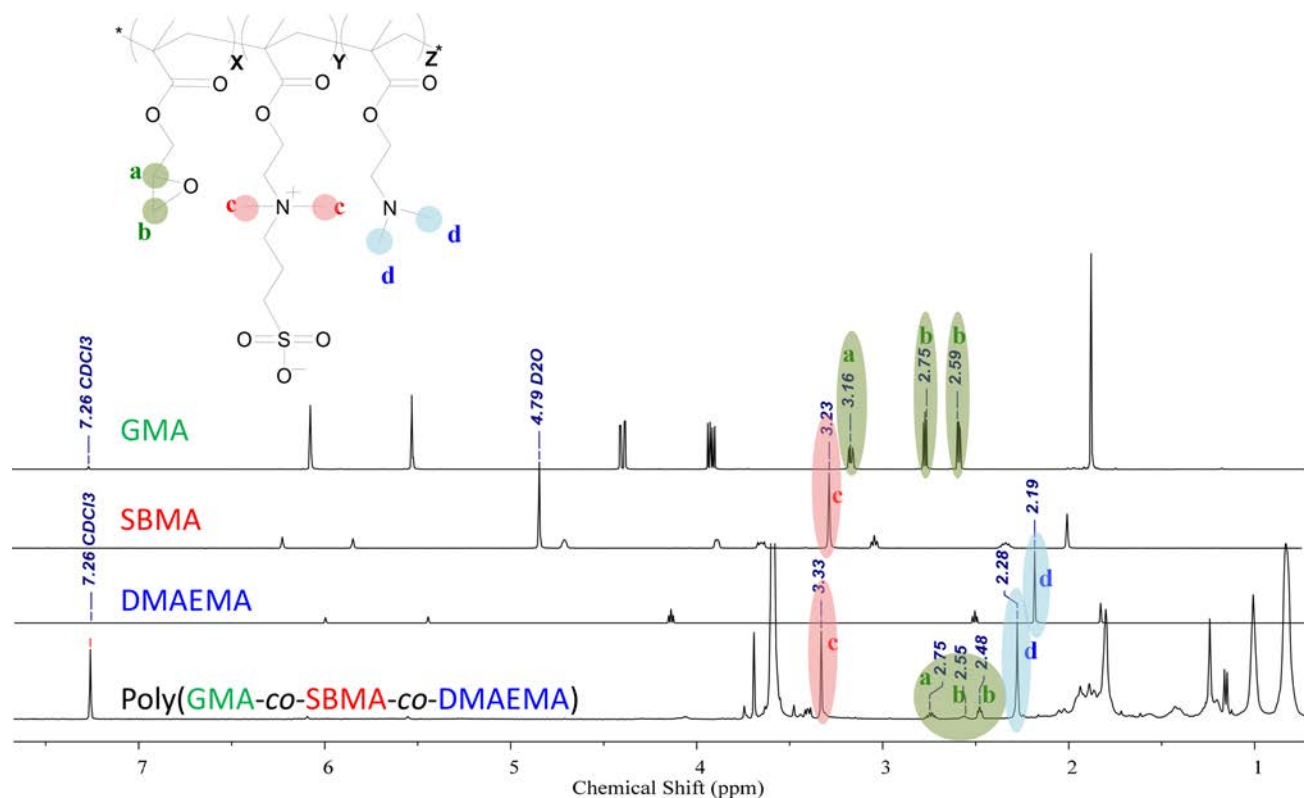


Figure 1. ^1H NMR spectrum of GMA, SBMA, and DMAEMA monomers, and poly(GMA-co-SBMA-co-DMAEMA) copolymer. The solvent was *d*-chloroform except for SBMA monomer for which D_2O was used.

property was the main aspect of this procedure, the pH-responsive G20-D80 was added as a control to monitor the pH dependence of poly(GMA-co-SBMA-co-DMAEMA). The quantitative results for the adhered and detached bacteria were determined using ImageJ cell counting software.

Surface Wettability and Morphology at Different pH. To assess the surface wettability of the grafted substrates at different pH, alternating water contact angles were measured at room temperature using a contact angle meter (Contact Angle DataPhysics OCA 20). First, the virgin and grafted PDMS substrates were immersed at pH 7.35 for 2 h. The substrates were dried with N_2 gas, and the water contact angle measured. The substrates were then dried with N_2 gas and immersed at pH 1.65 for 2 h. The substrates were then dried and their water contact angle measured. This tests was also carried out with pH 10 and pH 7.35 solutions. The alternating contact angle values were determined for 9 cycles. To determine the water contact angles from acidic to basic conditions, pH 7.35 was used as a starting pH between transitioning from pH 1.65 to 10.

The surface morphology of the surfaces was determined using an atomic force microscope (JPK NanoWizard3 Bioscience AFM with Zeiss AxioObserver RX) at room temperature. The grafted substrates were first immersed in pH 1.65 and 10 for 2 h at 37°C . A triangular-shaped Si cantilever with commercial tips (Olympus Co., Ltd.) of about 320 kHz resonance frequency from JPK was used to acquire the images in noncontact mode. The normal spring constant of the cantilever was 0.02 N/m. The force between the tip and the sample was 0.87 nN.

RESULTS AND DISCUSSION

Synthesis and Chemical Characterization of Poly(GMA-co-SBMA-co-DMAEMA) Copolymers. The experimental molar ratio obtained from ^1H NMR spectra are summarized in Table 1 while Figure 1. displays the peaks corresponding to the chemical structure of the poly(GMA-co-SBMA-co-DMAEMA) copolymer as well as those of GMA,

SBMA and DMAEMA monomers. The two small peaks at 2.55 and 2.75 ppm signify the presence of the epoxy side groups of the GMA segment while peak signals corresponding to methyl protons $(\text{CH}_3)_2\text{N}^+$ of SBMA units ($\delta = 3.33$ ppm) and $-\text{N}(\text{CH}_3)_2$ of the DMAEMA units ($\delta = 2.28$ ppm) were also identified on the spectrum of the copolymer. Therefore, we could confirm from the ^1H NMR characterization that the copolymer synthesized contained the three different units, GMA, SBMA and DMAEMA. Notice also that small peaks could be seen on the spectrum of poly(GMA-co-SBMA-co-DMAEMA) at δ ranging between 1 and 2 ppm, probably attributed to partial ring opening of epoxy groups of GMA units, or to remaining impurities. In Table 1, the theoretical and experimental molar ratio of the poly(GMA-co-SBMA-co-DMAEMA) copolymers were also calculated according to these peaks. It was found that the actual composition of the copolymers corresponded fairly well to their theoretical compositions. It indicates that the copolymerization reaction was well controlled and that the monomers had a similar reactivity during the synthesis.

Optimization of the Grafting Onto Procedure. Since PDMS surface is composed of unreactive siloxane bonds, activation of the surface is needed to generate anchoring functional groups such as hydroxyl groups. Surface hydroxylation can be done by UV/ozone. However, the UV/ozone process time needed to be optimized. In this respect, we studied the effect of the treatment time on the water contact angle in air of the activated surfaces, because UV/ozone arises in the formation of hydroxyl bonds, expected to enhance the surface hydrophilicity of the materials. Figure 2a shows that a treatment time of 30–35 min permitted to decrease the WCA from 112° (untreated PDMS) to 100° , but further increasing

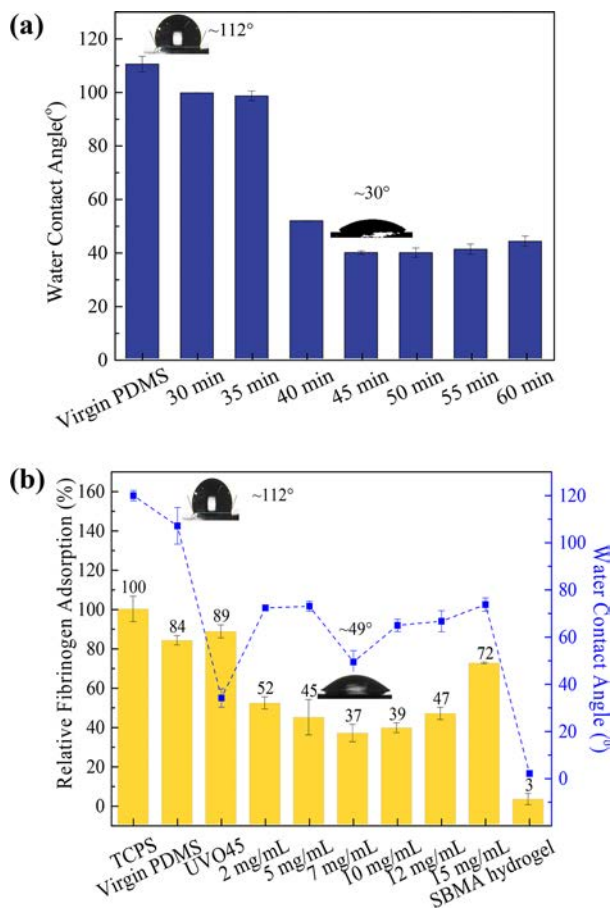


Figure 2. Optimization of (a) UV/ozone pretreatment time and (b) coating concentration of PDMS grafted with poly(GMA-*co*-SBMA-*co*-DMAEMA) with copolymer ratio of G20-S40-D40 after 45 min UVO pretreatment with TCPS and SBMA hydrogel as negative and positive controls.

the time to 40 min led to a drastic reduction of the WCA, as it was measured to be 50°. The WCA then continued to decrease a little bit and remained in the same range as a plateau was reached in the range 40°–45°, when increasing the time up to 60 min. Setting the UV/ozone treatment time to 45 min guarantees the formation of hydroxyl bonds necessary to the establishment of covalent bonds with the polymer. However, using UV/ozone for a very long time can cause a change in the mechanical strength of the PDMS substrate with a loss of its elastic modulus,³⁶ as well as it can alter its optical properties and in particular its transparency.³⁷ Based on these reported observations and because increasing the treatment time to 50, 55, or 60 min did not permit improvement of the surface hydrophilicity, 45 min was fixed as the UV/ozone treatment time for all experiments. One also has to note that no change in mechanical/optical property was visually noticed for a 45 min treatment time.

Once the optimum pretreatment time determined, another critical parameter that will later on determine the propensity of the grafted copolymer to mitigate biofouling is the coating concentration in the coating bath. In this respect, the effect of the concentration of poly(GMA-*co*-SBMA-*co*-DMAEMA) in the coating solution on the surface hydrophilicity and resistance to fibrinogen adsorption was also observed, and related results are reported in Figure 2b. Increasing the concentration up to 7 mg/mL showed better resistance against

adsorbed proteins and an increase in the hydrophilic property, compared to the virgin PDMS surface. A lower WCA, compared to that of the virgin PDMS, does not guarantee that the copolymer was successfully grafted onto the PDMS surface since activated PDMS surfaces also presented a very low WCA (Figure 2a), but the improved resistance to fibrinogen adsorption is a clear indication of the presence of the SBMA segments necessary for antifouling resistance, even though further chemical analyses are necessary. The formation of hydroxyl groups on the PDMS surface alone could not lead to better fouling mitigation, as it has been suggested from past studies that fibrinogen binds tightly to hydroxyl-grafted surfaces.³⁸ In general, we noticed that coating the copolymer actually resulted in higher WCAs than measured after surface activation. We hypothesized that the activation did not affect the surface structure that remained homogeneous and smooth, while the coating led to local rugosities, affecting the roughness of the surfaces and as a consequence, their wettability. This will be checked later in this manuscript. Then, increasing the concentration resulted in an increase in hydrophobicity and in surface fouling. This could be due to the deposition of unreacted poly(GMA-*co*-SBMA-*co*-DMAEMA) on the surface, or to the formation of multilayer coating as a random copolymer was at play, which hindered the antifouling properties of the modified PDMS.

Chemical Characterization of Poly(GMA-*co*-SBMA-*co*-DMAEMA)-Grafted PDMS Surfaces. The surface chemistry of grafted surfaces was analyzed by FT-IR and XPS, to confirm the presence of poly(GMA-*co*-SBMA-*co*-DMAEMA). The FTIR spectra are presented in Figure 3a. The presence of an intense band at 1720 cm⁻¹, assigned to the O=C=O ester band, signifies the presence of the copolymer as all three units, SBMA, GMA and DMAEMA, possess this functional group. The presence of PDMAEMA units is further verified from the two adsorption peaks at 2840 and 2906 cm⁻¹, associated with the C-H stretch of the -N(CH₃)₂ group. Increasing DMAEMA content in the copolymer results in higher absorbance at these bands. Simultaneously, there is a decrease of the -CH₃ signal at 1262 cm⁻¹ peak due to the oxidative conversion of Si-CH₃ after grafting.

However, the asymmetric and symmetric vibrations of the sulfonyl group (-SO₃⁻) of the SBMA segment that should normally be found at $\nu = 1180$ and 1020 cm⁻¹ cannot be seen due to the high transmittance of siloxane bonds present around the same region at 1020–1100 cm⁻¹.³⁹ We acknowledge that the presence of SBMA units cannot be ascertained from this FT-IR analysis, but as we proved (i) that the copolymer contained SBMA units (from Figure 1) and (ii) that the copolymer was grafted from the presence of the C=O stretch, then it can be concluded that SBMA is present at the surface of the PDMS grafted surfaces. Notice also that the results of Figure 2b indicated the presence of SBMA units without which a decrease in fibrinogen adsorption could not have been found. However, we pushed further the analysis and carried out XPS tests.

In Figure 3b, the PDMS grafted with poly(GMA-*co*-SBMA-*co*-DMAEMA) exhibited peaks at about 284.76, 286.26, and 288.56 eV which corresponds to the C-H, O=C-O, and C-O-C species in the C 1s core-level spectra, respectively. The spectra obtained are all very similar for the three copolymers tested because the three units (GMA, DMAEMA, and SBMA) contain these functional groups. The presence of SBMA units could be ascertained from the analysis of the N 1s core-level

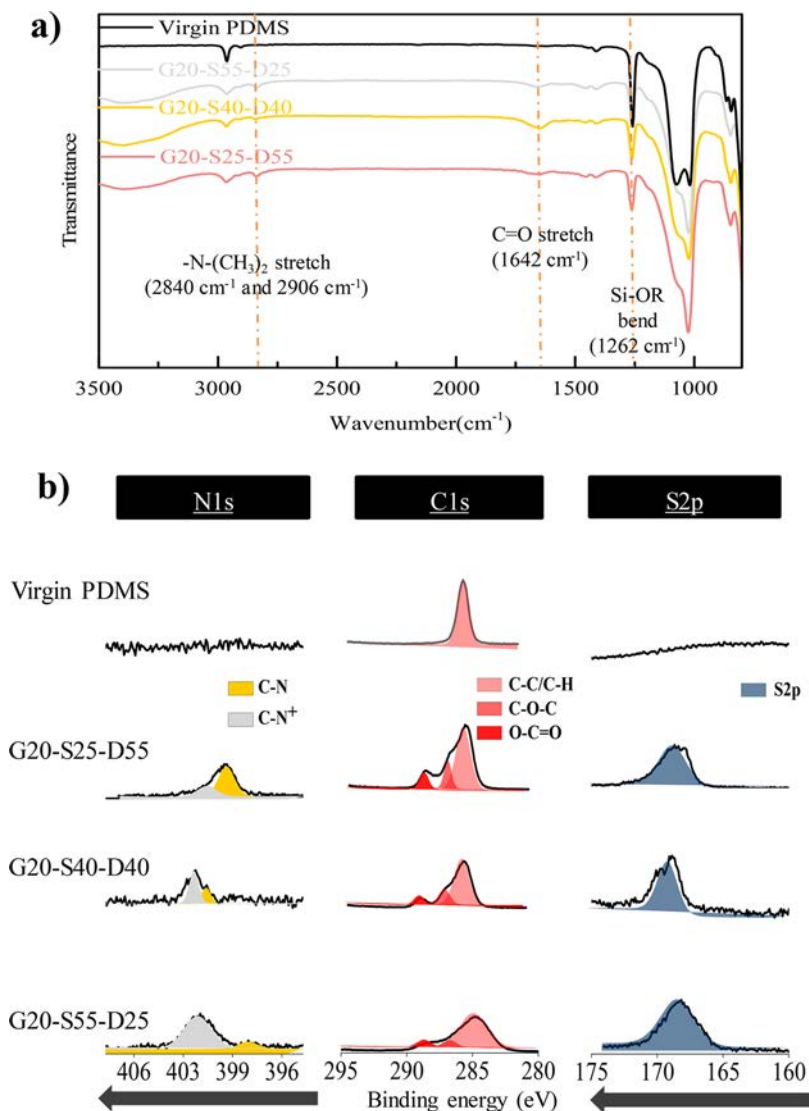


Figure 3. (a) FTIR spectra and (b) XPS spectra of virgin and PDMS grafted with G20-S25-D55, G20-S40-D40, and G20-S55-D25 surfaces.

spectra. Indeed, a signal at 400.89 eV, corresponding to the quaternary ammonium functional group, was clearly identified. But DMAEMA also partially contributed to this signal. Therefore, the S 2p core-level spectra were also determined. A peak was present at BE = 169 eV, confirming the presence of S=O and S-O species attributed to the SBMA segment.

In addition, the zeta potential of the grafted PDMS samples was assessed at different pH values. The results in Figure 4 reveal that the surface charge of virgin and grafted PDMS changes from acidic to basic conditions. Virgin PDMS has an overall negative zeta potential which might be due to the preferential adhesion of negative anions from the electrolyte solution over most of the pH range.⁴⁰ Surprisingly, the zeta potential of PDMS grafted with G20-S80 became negative in pH 5.5. Theoretically, the overall charge of the SBMA segment should be zero. But Guo et al. reported an overall negative surface charge of PSBMA from pH 5 to 10. They explained that the sulfonate groups acted as a strong acid ($pK_a = 2$) while the quaternary ammonium groups acted as a weak base ($pK_b = 5$).⁴¹ This gives PSBMA an overall acidic nature with an isoelectric point of 5.5, and so, it exhibits a slightly negative surface charge in basic conditions. On the other hand, the

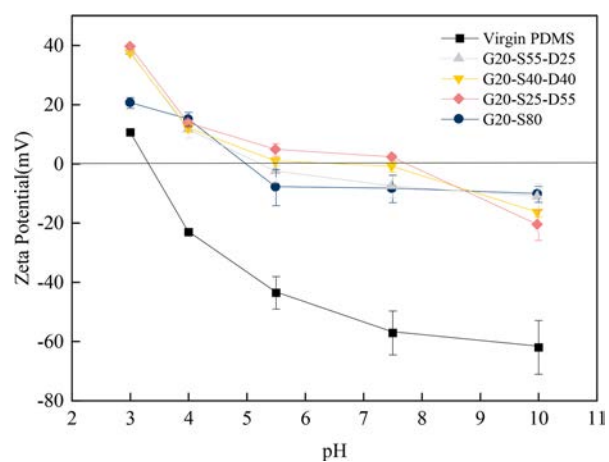


Figure 4. Zeta potential of virgin and PDMS grafted with different copolymer compositions of poly(GMA-co-SBMA-co-DMAEMA) and poly(GMA-co-SBMA).

increasing of PDMAEMA content in the copolymer led to a positive zeta potential at pH 3. It fell to 0 mV in neutral conditions, close to the isoelectric point of PDMAEMA

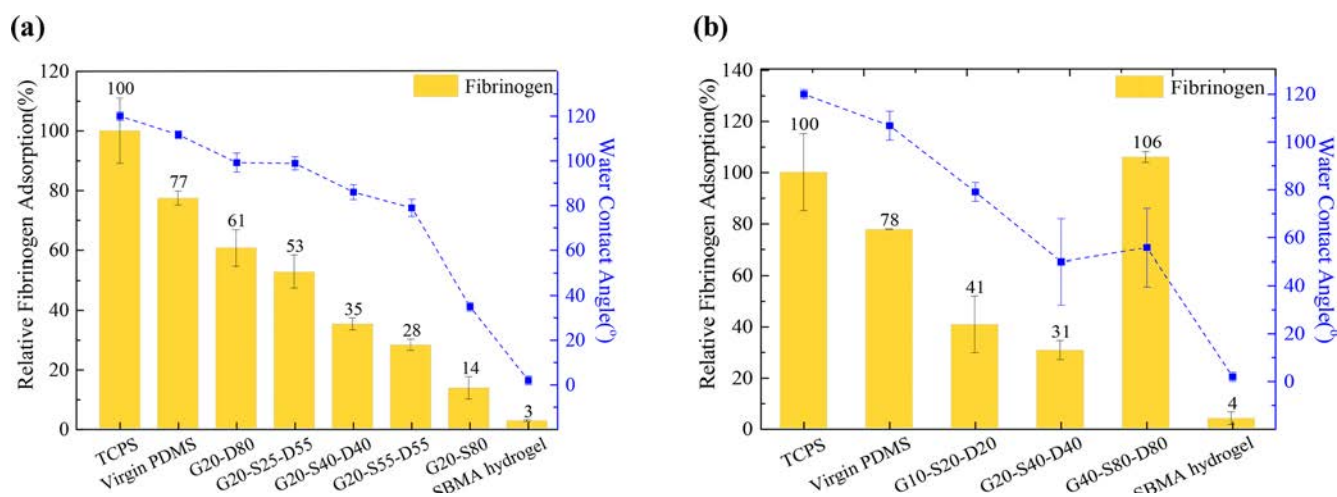


Figure 5. Effect of (a) different copolymer compositions and (b) copolymer chain length on fibrinogen adsorption and water contact angle of the different surfaces.

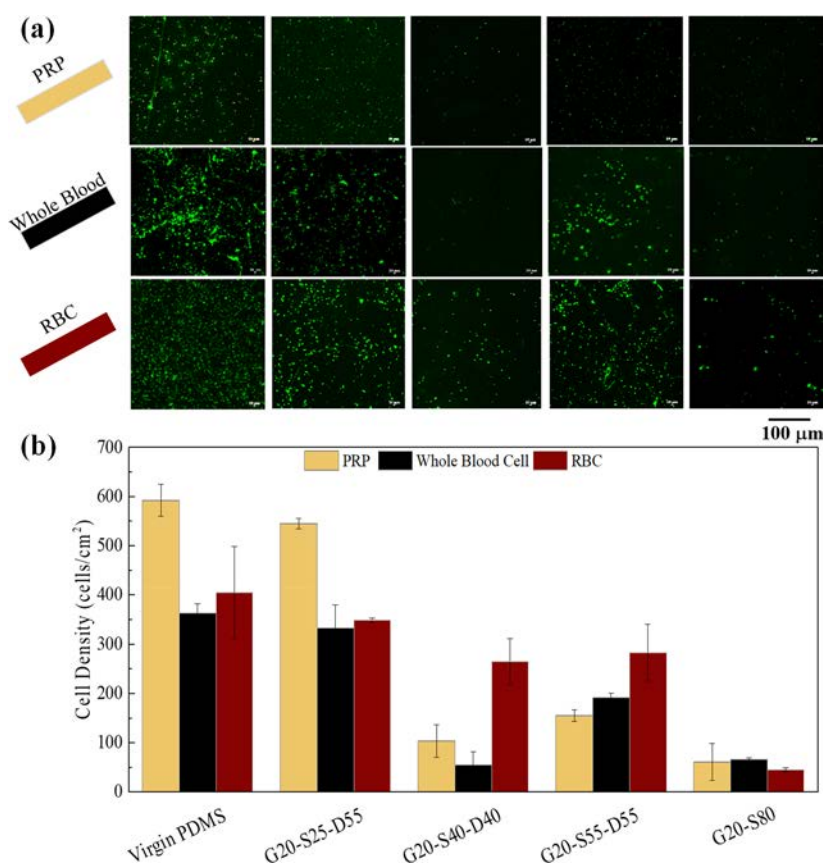


Figure 6. (a) CLSM image and (b) density of platelets, cells from whole blood, and erythrocytes on virgin and PDMS grafted with poly(GMA-*co*-SBMA-*co*-DMAEMA) and poly(GMA-*co*-SBMA) copolymers.

(7.4).³² Above pH 7.4, deprotonation of the tertiary amine of PDMAEMA resulted to a negative zeta potential due to the continuous absorption of negative ions onto the slipping plane of the uncharged surface of the grafted PDMS.⁴² This change from positive to negative zeta potential of grafted PDMS with varying PDMAEMA and PSBMA segment might be able to control the deposition and self-cleaning of cells onto biosensors in cell analysis applications.

Effect of the Copolymer Composition on the Grafted-PDMS Surface Wettability and on Their Resistance to

Nonspecific Protein Adsorption. We presented in previous section the optimization of the grafting process. But other than the process conditions, the copolymer composition and copolymer chain length are likely to influence the wettability and the antifouling properties of the grafted surfaces. Therefore, we grafted copolymers having different compositions and molecular weights onto PDMS surfaces, and determined the water contact angle and the resistance to fibrinogen adsorption of the grafted surfaces. Figure 5 shows the fibrinogen adsorption with respect to the surface

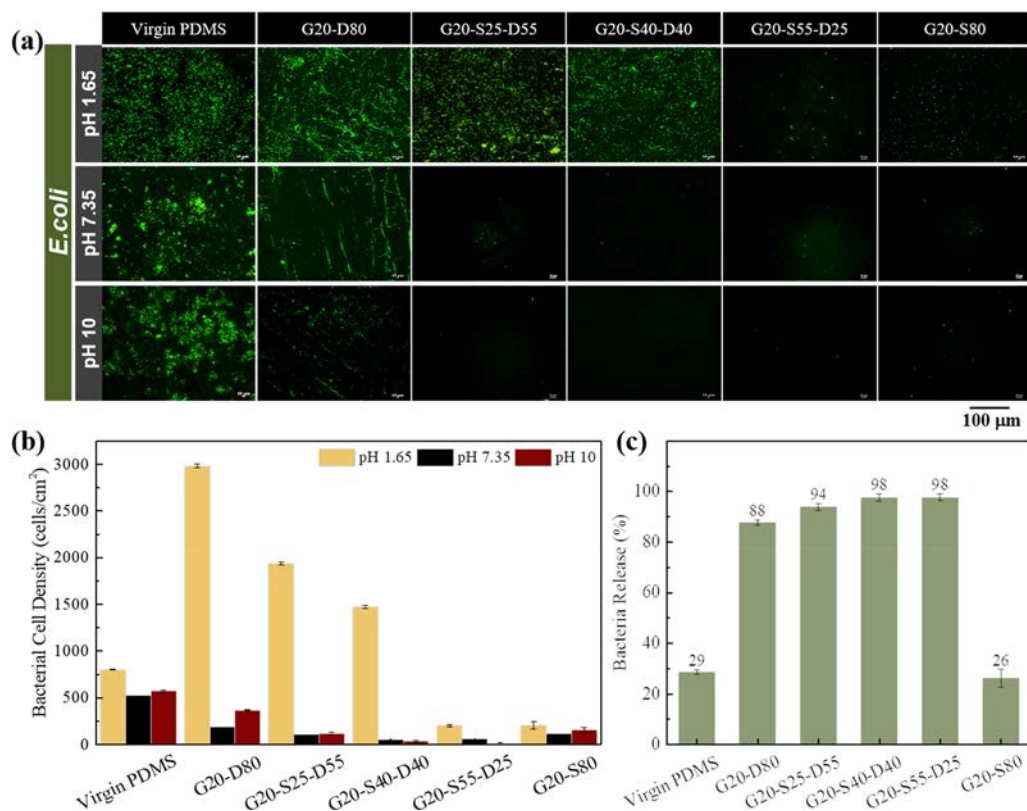


Figure 7. (a) CLSM image, attachment was performed at pH 1.65, and detachment at pH 7 and 10; (b) quantitative cell density; and (c) percentage of released bacteria after immersing virgin and grafted PDMS in pH 10 solution for 3 min.

hydrophilicity of the PDMS surface using 7 mg/mL as a fixed coating solution. In general, there is an increasing trend wherein increasing the SBMA content in the polymer chain decreases the protein adsorption and water contact angle on the surface. It was found in Figure 5a that the surface grafted with G20-S55-D25 permitted a decrease fibrinogen adsorption by 49%, compared with the virgin PDMS surface. Similarly, as the SBMA content in the copolymer increased, the WCA was found to keep on decreasing. Both results are clearly correlated and numerous previous studies starring SBMA-based polymers stressed on the importance of the formation of a tight hydration layer for surfaces to resist fibrinogen adsorption.^{41–43} Furthermore, G20-S25-D55 and G20-S40-D40 showed high amounts of protein adsorption compared to G20-S55-D25. This might be due to the electrostatic interaction of negatively charged fibrinogen⁴⁴ and positively charged PDMAEMA segment which correlates with the positive zeta potential of these copolymers in physiological pH that drives the adsorption of protein onto the surface.

The present results highlight that some particular copolymer compositions can seriously mitigate fibrinogen adhesion, and so may help at preventing events mediated by fibrinogen adsorption, such as thrombosis. In addition, Figure 5b shows distinctive results whether a short (G10-S20-D20), intermediate-length (G20-S40-D40), or long (G40-S80-D80) copolymer is used. In general, shorter (G10-S20-D20) and longer (G40-S80-D80) copolymers showed increased fibrinogen adsorption. In the case of G10-S20-D20 copolymer, the antifouling SBMA sequence is not long enough to ensure high coverage of the surface. In the case of high molecular weight copolymer (G40-S80-D80), (i) a decrease in chain flexibility may have ultimately compromised biofouling resistance, because not all

antifouling moieties could spread and participate in the formation of the protective hydration layer at the interface and (ii) the length of DMAEMA segment was too long, leading to enhanced interactions with the protein.

Effect of the Copolymer Composition on the Hemocompatibility of the Grafted-PDMS Surfaces.

Plasma protein adsorption and blood cell adhesion experiments aim at evaluating the hemocompatibility of the grafted PDMS substrates. After studying the effect of the copolymer grafting on the surface resistance to fibrinogen adsorption, we moved onto the assessment of their resistance to red blood cells, platelets and whole blood.

Figure 6 shows the CLSM confocal image and quantitative adhesion data of virgin and grafted PDMS substrates with poly(GMA-*co*-SBMA-*co*-DMAEMA) and poly(GMA-*co*-SBMA). As expected, high amounts of adhered platelets, cells from whole blood, and erythrocytes are observed on virgin PDMS samples. The results also indicated that the grafting of the copolymers led to a significant reduction of blood cells adhesion. In addition, the grafting with G20-S40-D40 led to the best results. Even though G20-S55-D25 possesses a higher SBMA content, the surface grafted with this copolymer did not perform as well in terms of resistance to blood cells, which was unexpected considering the results of Figure 5 and the generally observed positive correlation between fibrinogen adsorption and blood cell adhesion to a surface.^{45,46} This might be due to differences in local chains organization and charge distribution. The results of Figure 4 indicate that the G20-S40-D40-grafted PDMS surface is neutral at pH 7.4 while the surface grafted with G20-S55-D25 bears a net negative charge at pH 7.4 (−7.7 mV), and previous research showed that blood cells had a higher

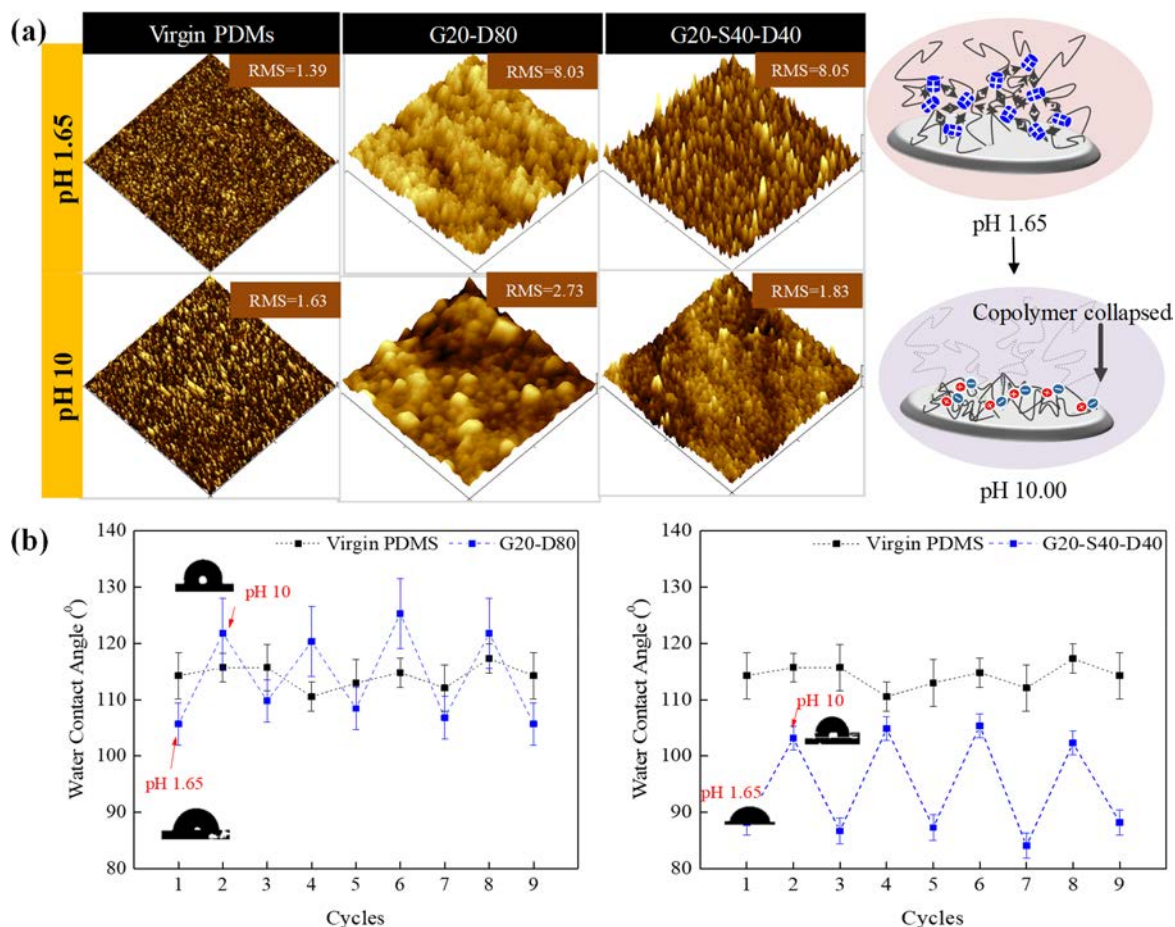


Figure 8. (a) Surface morphology and (b) wettability of virgin and PDMS grafted with G20-S40-D40 and G20-D80 in pH 1.65 and pH 10.

tendency to interact with negative surfaces than with a neutral and hydrophilic one, despite their net negative charge.⁴⁷

Effect of the Copolymer Composition on the Attachment/Detachment of Bacteria on/from the Grafted-PDMS Surfaces: Evaluation of the Self-Cleaning Ability of the Grafted Surfaces. To evaluate the self-cleaning performance of poly(GMA-co-SBMA-co-DMAEMA), an ideal polymer ratio that can both exhibit excellent fouling resistance and pH dependency should be identified. From the above results, poly(GMA-co-SBMA-co-DMAEMA) with 20% GMA, 40% SBMA and 40% DMAEMA referred to as G20-S40-D40 has shown to have excellent antifouling property. As it also possesses a significant amount of DMAEMA moieties, it should also exhibit pH-sensitive properties essential to the self-cleaning ability of the grafted surfaces.

In Figure 7a, bacterial attachment and detachment of virgin and grafted PDMS are shown. Since the isoelectric point of *E. coli* is about ~1.5, the lowest testing pH condition was chosen to be at pH 1.65 to ensure the negative charge of the bacterial medium.⁴⁸ Results showed that there is a higher bacterial attachment observed on PDMS grafted with copolymers with PDMAEMA segment at low pH. Since, DMAEMA has a pK_a of around 7.4,⁴⁹ it normally exists as a polycation in acidic environment which contributed to promote the surface attraction between the protonated $-NH^+(CH_3)_2$ of DMAEMA block and negatively charged bacterial surface as suggested from past studies.^{32,49} Also, as the content of SBMA increases in the copolymer, a decrease of bacterial attachment

is logically observed at low pH, consistent with the nonfouling nature of the zwitterionic segments.

Furthermore, the possibility to detach the adhered *E. coli* from the surface was investigated to show the self-cleaning performance of modified PDMS after immersing the grafted materials in aqueous bath at pH 7.35 and pH 10. In Figure 7b, immersing the samples at pH 7.35 already caused an appreciable decrease in bacterial cell density on modified PDMS. This might be due to the sudden decrease in surface potential as shown in Figure 4 which resulted to the repulsive interaction between the bacterial cell and the grafted PDMS. Additionally, by further increasing the pH to 10, the bacterial detachment was measured to be around 98% for PDMS surfaces grafted with G20-S25-D55 and G20-S40-D40 (Figure 7c). However, G20-S25-D55 does not mitigate fouling as well as G20-S40-D40 which makes it less desirable as a coating agent for bacterial cell analysis materials. In bacterial cell analysis, the selectivity and sensitivity of the sensor is important which means that fouling of nontarget proteins and cells must be inhibited. Also, G20-S40-D40 showed better self-cleaning property compared to G20-S80. Upon immersing the surfaces in high pH bath, the deprotonation of the DMAEMA segments weakens and eventually annihilates the attractive electrostatic interactions between the bacterial and the surface, initially established at lower pH. As a result, bacterial detachment from the surface was observed. For G20S80, however, there is no or very little effect of the pH, since the grafted copolymer does not contain any pH-sensitive segments. The low detachment still measured (26%) is only

due to the fact that the bacterial species that managed to adhere to the surfaces in the first place weakly interacted with the material, as SBMA provided a strong hydration layer. Removing the surfaces from the low pH medium in order to immerse them in high pH medium caused local disturbance (convective flow) which was enough to cause the detachment of the few bacterial species that initially adhered.

The Effect of the pH on the Surface Wettability and Morphological Changes of the Grafted-PDMS Surfaces.

AFM was used to study the changes of surface morphology of the virgin and modified PDMS at pH 1.65 and pH 10. As shown in Figure 8a, the surface showed tall, conelike structures heterogeneously distributed over the entire substrate area at pH 1.65. When the substrates were immersed in a solution at pH 10 (above the pK_a), smaller peaks, resulting from the deprotonation of the amine groups and chain collapsing, were visible on the modified surfaces. The AFM images indicate that the G20-S40-D40 and G20-D80 undergo significant structural changes, as a result of the hydrophilic/hydrophobic transition of the DMAEMA segment. Furthermore, the water contact angle at pH 1.65 was measured at $86.4^\circ (\pm 1.6)$ on the rough G20-S40-D40-grafted surface (RMS = 8.05) and increased to $104.2^\circ (\pm 1.3)$ on the flatter G20-S40-D40-grafted surface at pH 10 (Figure 8b). Increasing the roughness of a surface enhances air entrapment, and so, leads to an increase in WCA. A reverse trend was clearly seen here, which implies that the change of pH strongly affected the polymer chains organization (chain collapsing versus chain spreading) and, as a result, the polymer–water interactions. More precisely, ionization of PDMAEMA segment is a key factor to consider here. In low pH, the tertiary amine of DMAEMA accepts a proton which leads to the formation of ionic bonds with water.⁵⁰ This leads to the polarization of the protonated tertiary amine which results to wetting of the surface grooves of grafted PDMS surface causing it to become more hydrophilic. Likewise, the tertiary amine will donate a proton in high pH which causes the deprotonation of the DMAEMA segment and promoting hydrophobic interaction with the water droplet, thus prompts the formation of air pockets between the grooves. The ionic interaction between the protonated tertiary amine and water has shown to provide better hydration in acidic conditions, despite exhibiting higher surface roughness (Figure 8a). As a result, the change in morphology arising from the change in surface chemistry will affect the amount of adhered bacteria on the surface, which can be rationalized as follows. The AFM images of G20D80- and G20-S40-D40-grafted surface show distinct topography. In Figure 8a, it is seen that the surface roughness of G20-D80-grafted surface at pH 10 is higher than that of G20-S40-D40-grafted surface. Surface topography and roughness influence the interactions with bacteria, as reported by Lorenzetti et al., who evidenced that bacteria preferentially deposited within the valleys of macroscopic grooves while microscopic grooves decreased the contact area between the bacteria and the coating, hence preventing bacterial adhesion.⁵¹ The groove density on the G20-S40-D40-grafted surface appeared to be higher than on the G20-D80-grafted surface, with smaller indents (smaller roughness coefficient), which decreased the possibility of bacterial physical entrapment on G20-S40-D40-grafted surface, while bacteria could more readily interact within the wide grooves of the G20-D80-grafted surface. This explains why the amount of bacteria released from G20-D80-grafted surface was less than from the G20-S40-D40-grafted PDMS. Furthermore, the addition of

PSBMA segment enhanced the hydrophilicity of G20-S40-D40-grafted PDMS compared to G20-D80-grafted PDMS. This also importantly contributes to the higher amount of released bacteria from G20-S40-D40-grafted PDMS. Finally, results also suggest that when exposed in basic conditions, PSBMA segment became more apparent after the collapse of DMAEMA segments, further contributing to the release of adhering bacteria from the surface.

CONCLUSIONS

In this study, a self-cleaning PDMS surface grafted with poly(GMA-*co*-SBMA-*co*-DMAEMA) with antifouling and pH-sensitive properties was prepared and characterized.

We first introduced a novel copolymer composed of anchoring glycidyl methacrylate (GMA) segments, antifouling sulfobetaine methacrylate (SBMA) segments, and pH-responsive 2-(dimethylamino)ethyl methacrylate (DMAEMA) segments, poly(GMA-*co*-SBMA-*co*-DMAEMA), capable of reversibly switching from positively to negatively charged with pH modulation.

Copolymers with a varying composition were grafted onto PDMS surfaces, and surface wettability as well as their biofouling by proteins and blood cells, and their self-cleaning properties were scrutinized. PDMS grafted with G20-S40-D40 polymer was able to allow the attachment of bacteria and their detachment from the grafted surface material by exhibiting both antifouling and pH-sensitive properties.

The reversible hydrophilic/hydrophobic transition of grafted PDMS was shown to be pH-dependent. Immersing the samples in acidic conditions resulted in the protonation of the tertiary amine in DMAEMA, which promoted polarization with water. This in turn induced ionic interactions with water droplet on the surface grooves and thereby enhanced the surface wettability. This reversible pH-dependent wettability behavior is thought to be responsible for bacterial attachment/release, although further cyclic biofouling tests are still necessary to further evidence the reusability of the materials.

Manipulating the pH gradient allows to control the bacterial attachment on and their detachment from poly(GMA-*co*-SBMA-*co*-DMAEMA)-grafted PDMS surfaces, which offers an opportunity for the development of smart reusable biomaterial interfaces for bacterial sensing devices.

AUTHOR INFORMATION

Corresponding Author

*E-mail: ychang@cycu.edu.tw. Phone: 886-3-265-4122. Fax: 886-3-265-4199.

ORCID

Antoine Venault: [0000-0002-0383-695X](https://orcid.org/0000-0002-0383-695X)

Yung Chang: [0000-0003-1419-4478](https://orcid.org/0000-0003-1419-4478)

Author Contributions

This manuscript was written through contributions of all authors.

Notes

The authors declare no competing financial interest.

ACKNOWLEDGMENTS

The authors would like to acknowledge the project of Outstanding Professor Research Program at Chung Yuan Christian University, the Ministry of Science and Technology and the Agence Nationale de la Recherche (MOST-ANR International Program: MOST 107-2923-E-033-001), and the

Changhua Christian Hospital (1060526) for their financial support.

■ REFERENCES

- (1) Ng, J. M. K.; Gitlin, I.; Stroock, A. D.; Whitesides, G. M. Components for Integrated Poly(dimethylsiloxane) Microfluidic Systems. *Electrophoresis* **2002**, *23*, 3461–3473.
- (2) Wong, I.; Ho, C. M. Surface Molecular Property Modifications for Poly(dimethylsiloxane) (PDMS) Based Microfluidic Devices. *Microfluid. Nanofluid.* **2009**, *7*, 291–306.
- (3) Toepke, M. W.; Beebe, D. J. PDMS Absorption of Small Molecules and Consequences in Microfluidic Applications. *Lab Chip* **2006**, *6*, 1484–1486.
- (4) Utrata-Wesolek, A. Antifouling Surfaces in Medical Application. *Polymer* **2013**, *58*, 685–695.
- (5) Fusetani, N. Biofouling and Antifouling. *Nat. Prod. Rep.* **2004**, *21*, 94–104.
- (6) Pei, X.; Ye, Q. Development of Marine Antifouling Coatings. In *Antifouling Surfaces and Materials: From Land to Marine Environment*; Zhou, F., Ed.; Springer Verlag: Berlin, Heidelberg, 2015; pp 135–149.
- (7) Bohnert, J. L.; Horbett, T. A.; Ratner, B. D.; Royce, F. H. Adsorption of Proteins from Artificial Tear Solutions to Contact Lens Materials. *Invest. Ophthalmol. Visual. Sci.* **1988**, *29*, 362–373.
- (8) Fonn, D. Targeting Contact Lens Induced Dryness and Discomfort: What Properties Will Make Lenses More Comfortable. *Optom. Vis. Sci.* **2007**, *84*, 279–285.
- (9) Santos, L.; Rodrigues, D.; Lira, M.; Oliveira, M.E.C.D.R.; Oliveira, R.; Vilar, E. Y.; Azeredo, J. The Influence of Surface Treatment on Hydrophobicity, Protein Adsorption and Microbial Colonisation of Silicone Hydrogel Contact Lenses. *Cont. Lens Anterior Eye* **2007**, *30*, 183–188.
- (10) Liu, B.; Liu, X.; Shi, S.; Huang, R.; Su, R.; Qi, W.; He, Z. Design and Mechanisms of Antifouling Materials for Surface Plasmon Resonance Sensors. *Acta Biomater.* **2016**, *40*, 100–118.
- (11) Liu, X.; Huang, R.; Su, R.; Qi, W.; Wang, L.; He, Z. Grafting Hyaluronic Acid Onto Gold Surface to Achieve Low Protein Fouling in Surface Plasmon Resonance Biosensors. *ACS Appl. Mater. Interfaces* **2014**, *6*, 13034–13042.
- (12) Pirmoradi, F. N.; Jackson, J. K.; Burt, H. M.; Chiao, M. On-demand Controlled Release of Docetaxel from a Battery-less MEMS Drug Delivery Device. *Lab Chip* **2011**, *11*, 2744–2752.
- (13) Pirmoradi, F. N.; Ou, K.; Jackson, J. K.; Letchford, K.; Cui, J.; Wolf, K. T.; Gräber, F.; Zhao, T.; Matsubara, J. A.; Burt, H.; Chiao, M.; Lin, L. Controlled Delivery of Antiangiogenic Drug to Human Eye Tissue Using a MEMS Device. *Proc. IEEE Int. Conf. Micro Electro Mech. Syst.* **2013**, 1–4.
- (14) Tsai, N. C.; Sue, C. Y. Review of MEMS-based Drug Delivery and Dosing Systems. *Sens. Actuators, A* **2007**, *134*, 555–564.
- (15) Sundaram, H. S.; Ella-Menye, J.-R.; Brault, N. D.; Shao, Q.; Jiang, S. Reversibly Switchable Polymer with Cationic/Zwitterionic/Anionic Behavior Through Synergistic Protonation and Deprotonation. *Chem. Sci.* **2014**, *5*, 200–205.
- (16) Lowe, A. B.; McCormick, C. L. Synthesis and Solution Properties of Zwitterionic Polymers. *Chem. Rev.* **2002**, *102*, 4177–4189.
- (17) Ueda, T.; Oshida, H.; Kurita, K.; Ishihara, K.; Nakabayashi, N. Preparation of 2-Methacryloyloxyethyl Phosphorylcholine Copolymers with Alkyl Methacrylates and Their Blood Compatibility. *Polym. J.* **1992**, *24*, 1259–1269.
- (18) Zhou, R.; Ren, P. F.; Yang, H. C.; Xu, Z. K. Fabrication of Antifouling Membrane Surface by Poly(sulfobetaine methacrylate)/Polydopamine Co-deposition. *J. Membr. Sci.* **2014**, *466*, 18–25.
- (19) Wang, T.; Wang, Y. Q.; Su, Y. L.; Jiang, Z. Y. Antifouling Ultrafiltration Membrane Composed of polyethersulfone and sulfobetaine copolymer. *J. Membr. Sci.* **2006**, *280*, 343–350.
- (20) Mondal, S. Stimuli Responsive Surfaces for Fouling-resistant Polymeric Membranes. *J. Membr. Sci. Technol.* **2013**, *4*, 1–2.
- (21) Zheng, J.; Li, L.; Chen, S.; Jiang, S. Molecular Simulation Study of Water Interactions with Oligo (ethylene glycol)-terminated Alkanethiol Self-assembled Monolayers. *Langmuir* **2004**, *20*, 8931–8938.
- (22) Kim, M.; Schmitt, S. K.; Choi, J. W.; Krutty, J. D.; Gopalan, P. From Self-assembled Monolayers to Coatings: Advances in the Synthesis and Nanobio Applications of Polymer Brushes. *Polymers* **2015**, *7*, 1346–1378.
- (23) Yin, H.; Marshall, D. Microfluidics for Single Cell Analysis. *Curr. Opin. Biotechnol.* **2012**, *23*, 110–119.
- (24) Probst, C.; Grünberger, A.; Wiechert, W.; Kohlheyer, D. Polydimethylsiloxane (PDMS) Sub-micron Traps for Single-cell Analysis of Bacteria. *Micromachines* **2013**, *4*, 357–369.
- (25) Blainey, P. C. The Future is Now: Single-cell Genomics of Bacteria and Archaea. *FEMS Microbiol. Rev.* **2013**, *37*, 407–427.
- (26) Salih, N. M.; Sahdan, M. Z.; Morsin, M.; Asmah, M. T. Fabrication and Integration of PDMS-glass Based Microfluidic With Optical Absorbance Measurement Device for Coliform Bacteria Detection. *IFMBE Proc.* **2018**, *63*, 75–81.
- (27) Sidorenko, A.; Krupenkin, T.; Taylor, A.; Fratzl, P.; Aizenberg, J. Reversible Switching of Hydrogel-Actuated Nanostructures into Complex Micropatterns. *Science* **2007**, *315*, 487–490.
- (28) Sidorenko, A.; Krupenkin, T.; Aizenberg, J. Controlled Switching of the Wetting Behavior of Biomimetic Surfaces with Hydrogel-supported Nanostructures. *J. Mater. Chem.* **2008**, *18*, 3841–3846.
- (29) Sun, T.; Wang, G.; Feng, L.; Liu, B.; Ma, Y.; Jiang, L.; Zhu, D. Reversible Switching Between Superhydrophilicity and Superhydrophobicity. *Angew. Chem., Int. Ed.* **2004**, *43*, 357–360.
- (30) Makamba, H.; Kim, J. H.; Lim, K.; Park, N.; Hahn, J. H. Surface Modification of Poly(dimethylsiloxane) Microchannels. *Electrophoresis* **2003**, *24*, 3607–3619.
- (31) Lim, A. L.; Bai, R. Membrane Fouling and Cleaning in Microfiltration of Activated Sludge Wastewater. *J. Membr. Sci.* **2003**, *216*, 279–290.
- (32) Xiong, X.; Wu, Z.; Yu, Q.; Xue, L.; Du, J.; Chen, H. Reversible Bacterial Adhesion on Mixed Poly(dimethylaminoethyl methacrylate)/poly(acrylamidophenyl boronic acid) Brush Surfaces. *Langmuir* **2015**, *31*, 12054–12060.
- (33) Zengin, A.; Karakose, G.; Caykara, T. Poly(2-(dimethylamino)-ethyl methacrylate) Brushes Fabricated by Surface-mediated RAFT Polymerization and Their Response to pH. *Eur. Polym. J.* **2013**, *49*, 3350–3358.
- (34) Xu, F. J.; Cai, Q. J.; Li, Y. L.; Kang, E. T.; Neoh, K. G. Covalent Immobilization of Glucose Oxidase on Well-defined Poly(glycidyl methacrylate)-Si(111) Hybrids from Surface-initiated Atom-transfer Radical Polymerization. *Biomacromolecules* **2005**, *6*, 1012–1020.
- (35) Yu, B. Y.; Zheng, J.; Chang, Y.; Sin, M. C.; Chang, C. H.; Higuchi, A.; Sun, Y. M. Surface Zwitterionization of Titanium for A General Bio-inert Control of Plasma Proteins, Blood Cells, Tissue Cells, and Bacteria. *Langmuir* **2014**, *30*, 7502–7512.
- (36) Lötters, J. C.; Olthuis, W.; Veltink, P. H.; Bergveld, P. The Mechanical Properties of the Rubber Elastic Polymer Polydimethylsiloxane for Sensor Applications. *J. Micromech. Microeng.* **1997**, *7*, 145–147.
- (37) Zhou, J.; Ellis, A. V.; Voelcker, N. H. Recent Developments in PDMS Surface Modification For Microfluidic Devices. *Electrophoresis* **2010**, *31*, 2–16.
- (38) Martins, M. C. L.; Ratner, B. D.; Barbosa, M. A. Protein Adsorption on Mixtures of Hydroxyl- and Methyl-Terminated Alkanethiols Self-assembled Monolayers. *J. Biomed. Mater. Res.* **2003**, *67A*, 158–171.
- (39) Chou, Y. N.; Chang, Y.; Wen, T. C. Applying Thermosettable Zwitterionic Copolymers as General Fouling-resistant and Thermal-tolerant Biomaterial Interfaces. *ACS Appl. Mater. Interfaces* **2015**, *7*, 10096–100107.
- (40) Bračić, M.; Mohan, T.; Kargl, R.; Griesser, T.; Hribernik, S.; Köstler, S.; Stana-Kleinschek, K.; Fras-Zemljčić, L. Preparation of PDMS Ultrathin Films and Patterned Surface Modification with Cellulose. *RSC Adv.* **2014**, *4*, 11955–11961.

- (41) Guo, S.; Jańczewski, D.; Zhu, X.; Quintana, R.; He, T.; Neoh, K. G. Surface Charge Control for Zwitterionic Polymer Brushes: Tailoring Surface Properties to Antifouling Applications. *J. Colloid Interface Sci.* **2015**, *452*, 43–53.
- (42) Ye, H.; Huang, L.; Li, W.; Zhang, Y.; Zhao, L.; Xin, Q.; Wang, S.; Lin, L.; Ding, X. Protein Adsorption and Desorption Behavior of a pH-responsive Membrane Based on Ethylene Vinyl Alcohol Copolymer. *RSC Adv.* **2017**, *7*, 21398–21405.
- (43) Zhao, Y. H.; Wee, K. H.; Bai, R. Highly Hydrophilic and Low-protein-fouling Polypropylene Membrane Prepared by Surface Modification with Sulfobetaine-based Zwitterionic Polymer Through a Combined Surface Polymerization Method. *J. Membr. Sci.* **2010**, *362*, 326–333.
- (44) Żeliszewska, P.; Bratek-Skicki, A.; Adamczyk, Z.; Ciesla, M. Human Fibrinogen Adsorption on Positively Charged Latex Particles. *Langmuir* **2014**, *30*, 11165–11174.
- (45) Sin, M. C.; Chen, S.-H.; Chang, Y. Hemocompatibility of Zwitterionic Interfaces and Membranes. *Polym. J.* **2014**, *46*, 436–443.
- (46) Chang, Y.; Shu, S. H.; Shih, Y. J.; Chu, C. W.; Ruaan, R. C.; Chen, W. Y. Hemocompatible Mixed-charge Copolymer Brushes of Pseudozwitterionic Surfaces Resistant to Nonspecific Plasma Protein Fouling. *Langmuir* **2010**, *26*, 3522–3530.
- (47) Venault, A.; Hsu, K. J.; Yeh, L. C.; Chinnathambi, A.; Ho, H. T.; Chang, Y. Surface Charge-bias Impact of Amine-contained Pseudozwitterionic Biointerfaces on the Human Blood Compatibility. *Colloids Surf., B* **2017**, *151*, 372–383.
- (48) Hairden, V. P.; Harris, J. The Isoelectric Point of Bacterial Cells. *J. Bacteriol.* **1953**, *65*, 198–202.
- (49) Liu, S.; Armes, S. P. Polymeric Surfactants for the New Millennium: A pH-Responsive, Zwitterionic, Schizophrenic Diblock Copolymer. *Angew. Chem., Int. Ed.* **2002**, *41*, 1413–1416.
- (50) Yi, Z.; Zhu, L. P.; Zhao, Y. F.; Wang, Z. B.; Zhu, B. K.; Xu, Y. Y. Effects of Coagulant pH and Ion Strength on the Dehydration and Self-assembly of Poly(N, N-dimethylamino-2-ethyl methacrylate) Chains in the Preparation of Stimuli-responsive Polyethersulfone Blend Membranes. *J. Membr. Sci.* **2014**, *463*, 49–57.
- (51) Lorenzetti, M.; Dogša, I.; Stošicki, T.; Stopar, D.; Kalin, M.; Kobe, S.; Novak, S. The Influence of Surface Modification on Bacterial Adhesion to Titanium-based Substrates. *ACS Appl. Mater. Interfaces* **2015**, *7*, 1644–1651.